

RESEARCH ARTICLE

Gene expression and adaptive evolution of *ZBED1* in the hibernating greater horseshoe bat (*Rhinolophus ferrumequinum*)

Yanhong Xiao¹, Yonghua Wu^{1,2,*}, Keping Sun¹, Hui Wang¹, Tinglei Jiang¹, Aiqing Lin¹, Xiaobin Huang¹, Xinke Yue¹, Limin Shi³ and Jiang Feng^{1,*}

ABSTRACT

Mammalian hibernators experience physiological extremes, e.g. ischemia, muscle disuse and hypothermia, which are lethal to non-hibernators, implying the existence of underlying mechanisms that allow hibernators to withstand these physiological extremes. Increased cell proliferation is suggested to be such a strategy, but its molecular basis remains unknown. In this study, we characterized the expression pattern of *ZBED1* (zinc finger, BED-type containing 1), a transcription factor that plays a crucial role in regulating cell proliferation, in five tissues of the greater horseshoe bat (*Rhinolophus ferrumequinum*) during pre-hibernation, deep hibernation and post-hibernation. Moreover, we investigated the *ZBED1* genetic divergence from individuals with variable hibernation phenotypes that cover all three known mtDNA lineages of the species. Expression analyses showed that *ZBED1* is overexpressed only in brain and skeletal muscle, not in the other three tissues, suggesting an increased cell proliferation in these two tissues during deep hibernation. Evolutionary analyses showed that *ZBED1* sequences were clustered into two well-supported clades with each one dominated by hibernating and non-hibernating individuals, respectively. Positive selection analyses further showed some positively selected sites and a divergent selection pressure among hibernating and non-hibernating groups of *R. ferrumequinum*. Our results suggest that *ZBED1* as a potential candidate gene that regulates cell proliferation for hibernators to face physiological extremes during hibernation.

KEY WORDS: Zinc finger BED-type containing 1, Cell proliferation, Gene expression, Adaptive evolution, Protective mechanism

INTRODUCTION

Hibernation is a strategy taken by hibernators to survive the pressures of a harsh environment such as low ambient temperature and/or scarce food availability (Wang et al., 1996). In order to survive, hibernators must suffer potential adverse effects induced by long periods of low body temperature, and repeated ischemia and perfusion, some of which are highly stressful and even lethal for non-hibernators (Carey et al., 2003). However, hibernators obviously have abilities to protect themselves from potential harm, and several underlying mechanisms are proposed, such as induced expression of stress (heat shock) proteins to combat cellular stress (Carey et al., 1999, 2000; Lei et al., 2014) and increased

protein–ubiquitin conjugate concentration to help degrade damaged proteins during hibernation (Carey et al., 2000).

Among the protective mechanisms that underlie tolerance of physiological extremes is increased cell proliferation (Cerri et al., 2009). Both the number of apoptotic cells and the number of cells that undergo proliferation in the main brain areas of hibernating frogs increase compared with cell numbers in active frogs, suggesting a compensatory effect of increased cell proliferation for increased apoptotic cells during hibernation (Cerri et al., 2009). During hibernation, it is stressful for cells to be exposed to low temperatures for long periods because of its effects on processes such as protein stability, membrane function, ATP synthesis, activity of key regulatory enzymes and cytoskeletal integrity (Kandror and Goldberg, 1997; Sonna et al., 2002). Additionally, ischemia-induced oxidative stress during hibernation is considered to play a crucial role in cell death (Dave et al., 2012). Because of the high risk of cell death, increased cell proliferation might be an important protective mechanism for hibernating mammals to cope with potential cell damage during hibernation.

ZBED1 (zinc finger, BED-type containing 1), also called DREF (DNA replication-related element-binding factor), is a transcription regulatory factor playing a key role in the control of cell proliferation (Matsukage et al., 2008). *ZBED1* regulates cell proliferation by controlling many cell proliferation-related genes, such as those encoding PCNA, Orc 2, DNA polymerase α 180 kDa and 73 kDa subunits, RFC140, raf, E2F, cyclin A and Skp A (Hirose et al., 1991, 1993; Ohno et al., 1996; Takahashi et al., 1996; Kandror and Goldberg, 1997; Ryu et al., 1997; Sawado et al., 1998; Phung Thao et al., 2006; Tsuchiya et al., 2007; Matsukage et al., 2008). To date, no study about the role of *ZBED1* in hibernation has been reported. Given the important role of *ZBED1* in cell proliferation, it can be hypothesized to be a potential factor for helping physiological adaptation in hibernators. If it is the case, an increased expression of *ZBED1* in tissues vulnerable to stresses induced by physiological extremes during hibernation would be expected and adaptive evolution of the *ZBED1* gene in hibernating taxa may occur compared with non-hibernating taxa.

The greater horseshoe bat *Rhinolophus ferrumequinum* Schreber 1774, has a wide distribution in China and is found from southern China to northern China, and three divergent mtDNA evolutionary groups (Northeast, Central-East, Southwest) are identified (Sun et al., 2013). The Northeast group, which is distributed in Northeast China, hibernates strictly from December to April during winter, whereas the Southwest group, which is distributed in Southwest China, where the weather is warm and food is available even during winter, is active year-round (Aulagnier et al., 2008). Many individuals in the Central-East group (e.g. Beijing and Jinan), also hibernate during winter. The different hibernation phenotypes therefore provide us with an ideal model system to study the potential role of *ZBED1* in hibernation.

¹Jilin Provincial Key Laboratory of Animal Resource Conservation and Utilization, Northeast Normal University, 2555 Jingyue Street, Changchun 130117, China.

²School of Life Sciences, Northeast Normal University, 5268 Renmin Street, Changchun 130024, China. ³School of Life Science, Yunnan Normal University, Chenggong District, Kunming 650500, China.

*Authors for correspondence (fengj@nenu.edu.cn; wuyh442@nenu.edu.cn)

Received 16 October 2015; Accepted 8 January 2016

In this study, we characterized relative mRNA expression levels of the *ZBED1* gene in five tissues including heart, kidney, brain, liver and skeletal muscle, from Northeast individuals of *R. ferrumequinum* during pre-hibernation, deep hibernation and post-hibernation, respectively. We also analyzed adaptive evolution of *ZBED1* based on individuals from all three mtDNA groups. We aimed to (i) determine the expression pattern of *ZBED1* in different tissues across the hibernation cycle and (ii) determine the potential genetic divergence and possible adaptive evolution of *ZBED1* between hibernating and non-hibernating groups of *R. ferrumequinum*.

MATERIALS AND METHODS

Gene expression analyses of *ZBED1*

Sample collection

A total of 16 female greater horseshoe bats, belonging to the Northeast group, were used in this study and these individuals were collected at different time points in the Jilin Province of Northeast China (Table 1). Three individuals were sampled in September in the Ground Cave (125°50'25"E, 41°4'8"N), referred to as pre-hibernation individuals. Three and five individuals were sampled in December and April, from the Ground Cave and Pigeon Cave (125°56'19"E, 41°28'29"N), respectively – referred to as deep hibernation individuals. Five bats were sampled in May from Pigeon Cave, referred to as post-hibernation individuals. The pre-hibernation individuals and post-hibernation individuals were active and had obvious responses to stimuli (sound, touch and light) and high body temperatures, whereas the deep hibernation individuals were in a torpid state, had no response to stimuli and body temperatures close to ambient temperature. All bats were killed by decapitation as soon as they were caught in the caves to ensure RNA profiles most representative of their active or hibernation state, as well as to minimize pain and suffering. Surgical procedures were promptly performed to protect RNA from degradation. Five tissue types (heart, kidney, brain, liver and skeletal muscle) of each animal were rapidly excised, flash-frozen in liquid nitrogen and then stored at -80°C until processed for RNA isolation. All experimental procedures carried out in this study were approved by the National Animal Research Authority of Northeast Normal University, China (approval number: NENU-20080416) and the Forestry Bureau of Jilin Province of China (approval number: [2006]178).

Total RNA isolation

Total RNA was isolated from bat tissues using TRIzol Reagent (Life Technologies, Carlsbad, CA, USA). Approximately 50 mg tissue was ground in liquid nitrogen using a pestle and mortar, and then solubilized in 1 ml ice-cold TRIzol reagent and incubated for 5 min. The cell debris was pelleted by centrifuging the homogenates at 12,000 *g* at 4°C for 10 min and 0.2 ml 100% chloroform was added

to the supernatant, then tubes were shaken vigorously by hand for 15 s and incubated at room temperature for 5 min. Then the aqueous phase was transferred to a fresh tube after centrifuging at 12,000 *g* at 4°C for 15 min and an equal volume of 100% chloroform was then added. After shaking tubes vigorously by hand for 15 s, they were incubated on ice for 2–3 min and centrifuged at 12,000 *g* at 4°C for 10 min to extract again. Next, 0.5 ml of isopropyl alcohol was added to the aqueous phase transferred into a fresh tube and the RNA was precipitated at -80°C overnight. The next day, the supernatant was removed from the tube after centrifugation at 12,000 *g* at 4°C for 10 min. Then the RNA pellet was washed with 1 ml of 75% ethanol by vortexing and centrifuging at 7500 *g*, 4°C for 5 min. Finally, the RNA pellet was air-dried for 5–10 min, and then dissolved in RNase-free water. Non-denaturing agarose gel electrophoresis and a NanoDrop spectrophotometer (Thermo Fisher Scientific, Waltham, MA, USA) were used to assess the quality and quantity, respectively, of the isolated RNA. $A_{260/280}$ values were all above 2.0 and electrophoresis of the RNA samples demonstrated that 28S and 18S rRNA were intact.

cDNA synthesis

A total of 80 RNA samples were converted to cDNA by using TransScript One-Step gDNA Removal and cDNA Synthesis SuperMix (TransGen Biotech, Beijing, China) following the manufacturer's instructions. The reaction mixture contained approximately 1 μg RNA template, 0.5 μg Anchored Oligo (dT)₁₈ primer and 6 μl RNase-free water and was incubated at 65°C for 5 min, then on ice for 2 min. In the next step, a mixture containing 2 \times TS Reaction Mix, TransScript RT/RI Enzyme Mix and gDNA Remover was added into the mixture from the first step. The final 20 μl reaction mixture was incubated at 42°C for 30 min, and finally 85°C for 5 min.

Real-time quantitative PCR

Quantitative RT-PCR was performed using StepOne Real-Time PCR System (Applied Biosystems) with an automatic threshold calculated by StepOne software v.2.1. The primer pairs of *ZBED1* and reference gene β -actin specified for *R. ferrumequinum* are listed in Table S1, including their sequences, annealing temperatures and product lengths. The efficiencies of these two genes are all approximately 100%, which ensures that the $\Delta\Delta\text{Ct}$ equation is used correctly. The total 10 μl PCR mixture contained 5 μl Thunderbird Sybr qPCR Mix (Toyobo), 0.2 μl 50 \times ROX reference dye, 1 μl cDNA template and 0.25 $\mu\text{mol l}^{-1}$ of each primer. The PCR was performed under the following conditions: pre-denaturation at 95°C for 1 min, then 40 cycles: 95°C, 15 s; 60°C for 1 min, with data collection after each cycle. Next is melting/dissociation curve analysis.

The relative quantity was calculated by using the $2^{-\Delta\Delta\text{Ct}}$ method (Livak and Schmittgen, 2001). The fold changes of *ZBED1* gene in five tissue types between September (pre-hibernation) and December (deep hibernation) were calculated relative to September; between April (deep hibernation) and May (post-hibernation) were calculated relative to April. The relative expression folds were expressed as mean \pm s.e. and statistical significance between active and torpid samples was analyzed using an independent-samples *t*-test. In further analysis, the fold changes of *ZBED1* in kidney, brain, liver and skeletal muscle were calculated relative to heart. The statistical significance among the five tissues was analyzed by one-way ANOVA followed by *post hoc* Tukey's test (SPSS v.19.0). Differences between means were statistically significant when $P < 0.05$.

Table 1. Sample information used for gene expression analyses

Sampling site	Sampling time	State	T_b (mean \pm s.d.)	<i>N</i>
Ground cave	September	Pre-hibernation (active)	34.6 \pm 0.6°C	3
Ground cave	December	Deep hibernation (torpor)	6.9 \pm 0.5°C	3
Pigeon cave	April	Deep hibernation (torpor)	8.4 \pm 0.3°C	5
Pigeon cave	May	Post-hibernation (active)	32.2 \pm 2.6°C	5

T_b , body temperature.

Adaptive evolution analyses of *ZBED1*

Samples collection, cloning and sequencing

Forty-six individuals of *R. ferrumequinum* were sampled from 13 different localities covering all three known mtDNA groups (Fig. 1, Table S2). One individual of *Rhinolophus macrotis* was also sampled to be used as an outgroup for phylogenetic analyses. Biopsy punches (3 mm diameter) were used to acquire bat wing membrane (plagiopatagium) samples as outlined by Worthington Wilmer and Barratt (1996). The 3 mm holes in each wing heal in ~4 weeks (Worthington Wilmer and Barratt, 1996). Genomic DNA was extracted from the wing biopsies using the Animal Genomic DNA Isolation Kit (Sangon, China). Primer pairs for amplification of *ZBED1* coding domain sequence (CDS) were designed according to cDNA sequence (KU312321) of *ZBED1* and whole genome shotgun sequence of *R. ferrumequinum* (Accession numbers: AWHA01106959.1 and AWHA01106960.1) using Primer Premier 5.0. Sense primer sequence was 5'-GCTGTTGTC-CTGCTT-3' and anti-sense primer sequence was 5'-ACCCCATCTGTCTGCTACT-3'. To reduce mutations introduced by amplification, Q5 super fidelity 2× Master Mix (Biolabs) was used according to the manual instructions. Purification of PCR product was completed by using a TaKaRa MiniBEST Agarose Gel DNA Extraction Kit. Cloning of *ZBED1* CDS was performed using a pEASY Blunt Zero Cloning Kit (TransGen Biotech). Five positive clones of each individual were randomly selected to be sequenced by Shanghai Sangon Biotechnology. All CDS sequences of *ZBED1* were deposited in GenBank with accession numbers KR868578–KR868649.

Data analyses

All 46 individuals sampled were sequenced successfully. Some individuals were determined to be heterozygotes and both allele sequences from the heterozygote individuals were used for subsequent analyses. Sequences were aligned using ClustalW implemented in MEGA 6 (Tamura et al., 2013). Polymorphic site detection and haplotype analysis were implemented in Dnasp 5.0 (Librado and Rozas, 2009). The sequence alignment was analyzed with RDP 3 (Martin et al., 2010), implementing several algorithms to detect recombinant sequences.

The phylogenetic relationship of the *ZBED1* gene was constructed using MrBayes 3.2.0 (Ronquist and Huelsenbeck,

2003). The DNA substitution model that best fit the data was estimated using the Akaike information criterion using Modeltest 3.7 (Posada and Crandall, 2005). Bayesian inference was run with four simultaneous chains, each of 1×10^6 generations, sampled every 100 generations and the first 25% of trees were discarded as 'burn-in'. The *ZBED1* CDS of *R. macrotis* was also cloned and sequenced, which was used as the outgroup.

The adaptive evolution of the *ZBED1* gene was determined by positive selection analyses. For this, the CODEML program in PAML package was used to derive maximum-likelihood estimates of the rate of nonsynonymous substitutions (d_N) and synonymous substitutions (d_S) (Yang, 2007). A d_N/d_S ratio (ω) of >1 signifies positive selection, a ratio of ~ 1 signifies neutrality and a ratio of <1 signifies purifying selection. Branch models, branch-site models, site-specific models (M1a, M2a, M3, M7, M8), and clade model (model C) were implemented in the CODEML program. Each model was fit to the data multiple times with different initial omega values to help ensure local optima were avoided. Likelihood ratio tests (LRTs) were used to compare the model fit of complex models against simpler, nested models. LRTs were carried out by comparing twice the difference in \ln likelihood scores of nested models against a χ^2 distribution with the degrees of freedom equal to the number of extra parameters estimated by the more complex model. The species tree was constructed based on the published mtDNA phylogenetic tree of *R. ferrumequinum* (Sun et al., 2013), and the inner relationships within each of the three mtDNA groups were respectively constructed using MrBayes 3.2.0 and nucleotide sequences of the *ZBED1* CDS. The best-fit models selected for 1st, 2nd and 3rd codon sites within the Northeast group were TIM, HKY and HKY, respectively. Similarly, the best-fit models selected for 1st, 2nd and 3rd codon sites within the Central-East and Southwest group were K81uf, TIM and HKY+I+G, and TIM, F81 and HKY+G, respectively. Based on the species tree, branch models were used to identify branches under positive selection. For this, a one-ratio model and a free-ratio model were initially employed, and then two-ratio models that assumed the positive selection of the ancestral branches of the Northeast group and the Central-East group of *R. ferrumequinum* were used, respectively. In addition, we also applied two-ratio models to the branches with $\omega > 1$ identified under the free-ratios model, which assumes an independent ω ratio for each branch, to identify potential positively selected branches in the phylogeny of *R. ferrumequinum*.

Branch-site models were applied to the ancestral branches of the Northeast and the Central-East groups to identify the certain sites under positive selection. Estimates of site-wise ω values in these foreground branches were then compared with estimates across the remaining background branches in the phylogeny. Under model A, the ω values were assigned to four predefined site classes. Site class 0 was estimated from data but constrained ($0 < \omega_0 < 1$), site class 1 $\omega_1 = 1$, site class 2a ω_{2a} could exceed 1 on the foreground but is constrained to be under purifying selection on the background, and site class 2b ω_{2b} could exceed 1 on the foreground but not on the background. The null model fixes $\omega_2 = 1$. The comparison between these two models is so-called test 2, with one degree of freedom (d.f.). In addition, test 1 was also used for the analyses, which compares model A with M1a (nearly neutral), with d.f.=2.

A clade model was applied to test potential divergent selection between hibernating and non-hibernating groups of *R. ferrumequinum*. We compared ω ratios averaged across branches within focal clades (foreground) with ω ratios estimated for the rest of the tree (background) (Bielawski and Yang, 2004). In clade models, we applied a 'multi-clade' approach, which allows for more than two

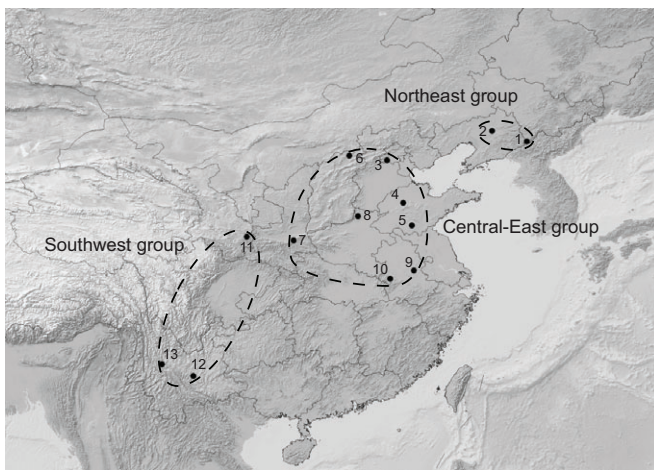


Fig. 1. Distribution of *R. ferrumequinum* sampling sites in China. The corresponding three mtDNA groups (Northeast, Central-East and Southwest) are outlined with dashed lines. Numbers 1–13 represent 13 isolated sampling sites.

tree partitions to examine complex patterns of divergence in selection across the phylogeny by comparing such models against simpler, nested models with fewer tree partitions (Weadick and Chang, 2012a). Models M1a and M2a_rel were used as null models for model C in LRTs. M1a is the standard null model for model C. However, model C versus M1a LRT was reported prone to false-positive test results when faced with moderate among-site variation in selective constraint (Weadick and Chang, 2012b). M2a_rel null model proposed by Weadick et al. (2012b) was therefore also used in this study.

Positively selected sites were analyzed using both PAML and HyPhy. With PAML, we compared site models M2a (selection) versus M1a (neutral), M7 (beta) versus M8 (beta and ω). We also compared models M3 (discrete) versus M0 (one ratio) to test change of ω ratio among sites. The Bayes empirical Bayes (BEB) was used to identify sites under positive selection. In HyPhy we used open-source software packages available under the datamonkey web-server (<http://www.datamonkey.org/>; Pond and Frost, 2005a,b; Pond and Muse, 2005; Murrell et al., 2012), to implement five different methods, including single-likelihood ancestor counting (SLAC), fixed-effects likelihood (FEL), random-effects method (REL), mixed-effects model of evolution (MEME) and fast unbiased Bayesian approximation (FUBAR).

RESULTS

Differential expression of *ZBED1*

The Northeast group of *R. ferrumequinum* is known to have a strict hibernation behavior during winter, and here we analyzed its *ZBED1* expression level in five different tissues across pre-hibernation, deep hibernation and post-hibernation. Three tissues (heart, kidney and liver) consistently presented a decreased expression during deep hibernation (December and April) compared with both pre-hibernation (September) and post-hibernation (May). By contrast, the two other types of tissue, brain and skeletal muscle, showed an increased expression during deep hibernation and decreased expression in both pre-hibernation and post-hibernation (Fig. 2A,B). However, only the expression differences of *ZBED1* in brain and skeletal muscle between April and May were statistically significant, with *P*-values of 0.011 and 0.017, respectively. The smaller sample size in September and December than in April and May may limit the statistical difference of *ZBED1* expression in brain and skeletal muscle between September and December.

We further analyzed the relative expression levels of *ZBED1* for each of the five tissue types and for the four time points (September, December, April and May) (Fig. 3). The results show that *ZBED1* was expressed most strongly in skeletal muscle compared with the other four tissues (Fig. 3). Liver showed the least expression (Fig. 3). Expression of *ZBED1* in kidney, brain and liver showed no significant difference at the three time points: May, December and April, with *P*-values >0.05 (Fig. 3B–D), except for expression at the active state in September, which showed significant differences among these three tissues (Fig. 3A). The differences in expression between heart and kidney were not significant at the four time points (Fig. 3).

Genetic analysis

Among 46 individuals analyzed, 26 individuals were determined to be heterozygous, and a total of 39 haplotypes were detected (Table S3). Among the 39 haplotypes, 64 polymorphic sites were found, of which 7 sites (1092, 1206, 1281, 1335, 1344, 1555 and 1626) were homozygous and identical between the Northeast group

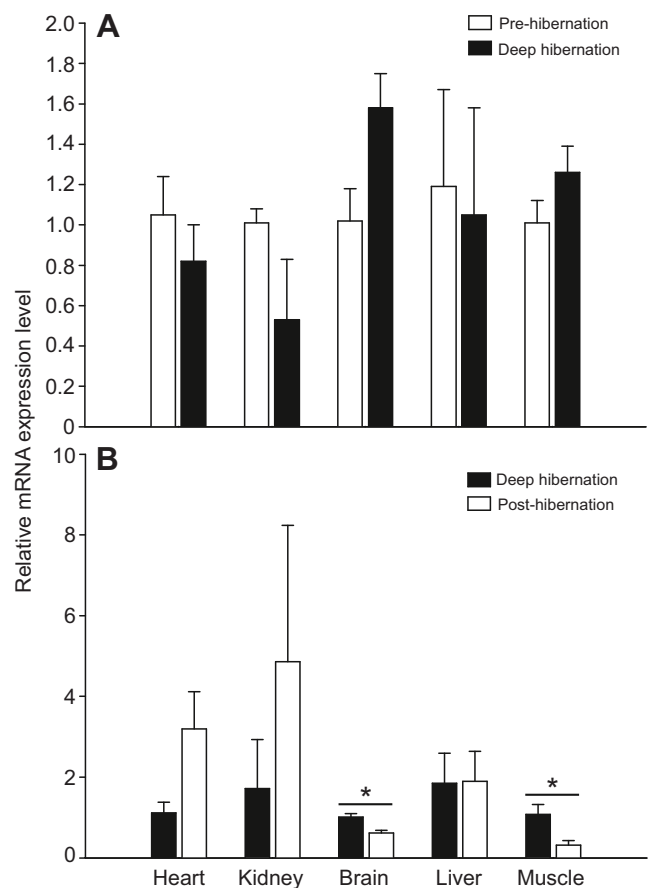


Fig. 2. Relative quantification of *ZBED1* gene expression in five tissues of *R. ferrumequinum*. mRNA expression was measured in heart, kidney, brain, liver and skeletal muscle from pre-hibernation (September) to deep hibernation (December) (A), and from deep hibernation (April) to post-hibernation (May) (B). The statistical significance was analyzed using an independent-samples *t*-test. Asterisks indicate significant differences between the two states ($P < 0.05$). Error bars indicate s.e.

and the Central-East group but different from the Southwest group (Table 2). No evidence of recombinant sequence was found in our dataset. To determine the genetic divergence of the *ZBED1* gene within the species, the Bayes tree based on the complete CDS of the *ZBED1* gene was constructed (Fig. 4A). The best-fit models for 1st, 2nd and 3rd codon sites were TIM, TIM and K81uf+I+G, respectively. Accordingly, 39 haplotypes of the *ZBED1* gene were clustered into two well-supported clades, with one clade containing only individuals from the Southwest group, and the other one containing individuals from both the Northeast group and the Central-East group. Unlike the mtDNA result, the haplotypes of the *ZBED1* gene from the Northeast group and the Central-East group did not form two clades, but were clustered into one clade.

Positive selection analysis

To determine the potential adaptive evolution of the *ZBED1* gene, different models implemented in PAML were employed. In branch models, the one-ratio model (M0) showed a single ω ratio ($\omega_0 = 0.01926$) for the entire tree (Table 3). The free-ratio model showed high variable ω ratios among branches, of which seven branches (a–g in Fig. 4B) were considerably higher than 1 (Table 3), although the LRT statistic of the free-ratio model versus the one-ratio model was not significant with $2\Delta l = 60.90$ ($P = 0.924$ and d.f. = 78). The seven branches were further designated as the

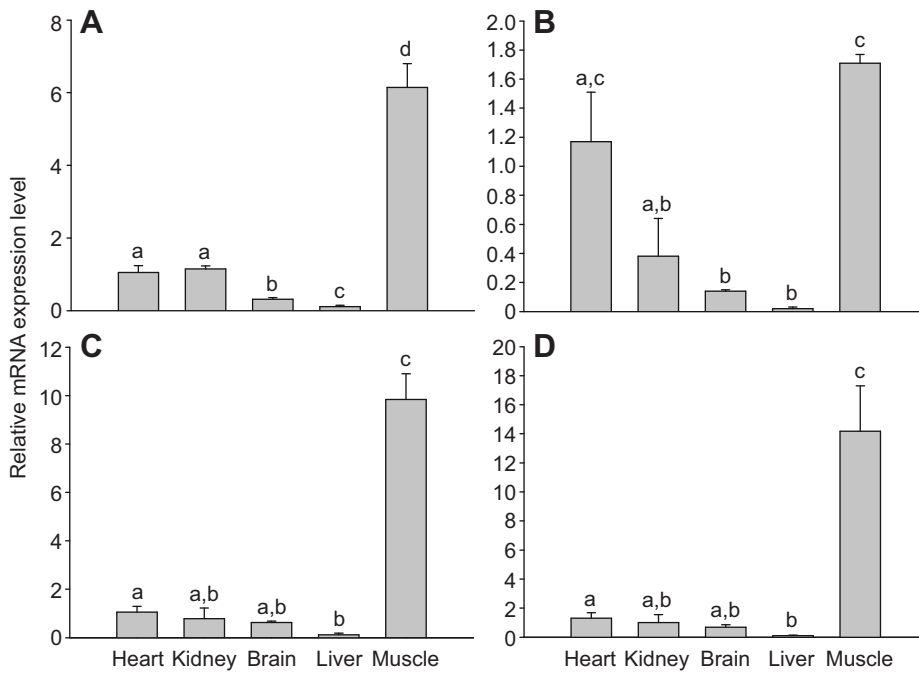


Fig. 3. Differential expression of the ZBED1 gene in different *R. ferrumequinum* tissues collected at different times. Samples were collected in September (A), May (B), December (C) and April (D). Individual mRNA expression values are normalized to the mean value in heart, and calculated as $2^{-\Delta\Delta Ct}$. Normalized mRNA expression values for multiple individuals were averaged by tissue. Different letters indicate significant differences among tissues (Tukey's test, $P < 0.05$). Error bars in the figure are s.e.

foreground branches and a two-ratio branch model was then analyzed (Table 3). Among seven branches, only five branches had a significantly better fit than the one-ratio model (Table 3). Interestingly, all these five branches belonged to the Northeast group and the Central-East group. To test whether the ancestral branches of the Northeast group (branch NE) and the Central-East group (branch CE) underwent positive selection, branches NE and CE were then respectively defined as foreground branches with others being background branches, and ω ratios of these two branches were calculated to be 2.01765 and 1.48366, respectively. The LRT statistic showed that the two-ratio models were not significantly better than the one-ratio model. We further used branch-site model A to identify possible positively selected sites of NE and CE branches. Whereas the LRT statistics of both test 1

and test 2 were not significant, the ω_{2a} and ω_{2b} ratios for the ancestral NE and CE branches were higher than 1 (Table 4).

Subsequently, different site-specific models (M1a, M2a, M3, M7 and M8) were further analyzed (Table 5). M2a (positive selection) identified one amino acid (324A) under positive selection at the 72.4% probability, whereas the LRT statistic of the M1a–M2a comparison was not significant ($P=0.664$). M8 showed that five sites were under positive selection with $\omega=1.00952$, and one (324A) of the five sites showed a high probability of 93.2%. The difference between M7 and M8 was statistically significant ($2\Delta l=13.70$, d.f.=2, $P=0.001$). The analyses based on datamonkey web-server also supported that amino acid 324A was under positive selection, because at least two methods, REL and FUBAR, significantly identified 324A to be under positive selection with $\omega > 1$ (Table S4).

Table 2. Single-nucleotide polymorphisms of ZBED1 CDS among three groups: Northeast, Central-East and Southwest

Group	Position of nucleotide															
	192	243	261	291	318	348	358	375	417	426	441	447	450	462	510	590
NE	C	G	C	C	G	G	G	Y	R	C	C	C	Y	C	Y	Y
CE	C	G	C	S	G	R	R	Y	R	Y	S	Y	Y	Y	Y	Y
SW	Y	R	Y	S	R	R	G	Y	G	C	C	C	Y	C	C	C
	609	633	654	675	683	684	693	699	714	728	735	750	759	768	774	810
NE	C	Y	G	C	C	C	T	C	C	Y	G	C	C	T	G	C
CE	C	Y	R	C	Y	C	T	Y	C	Y	G	C	S	Y	R	C
SW	Y	C	G	S	C	Y	Y	C	M	C	K	Y	C	C	G	Y
	837	855	894	934	954	964	971	979	1017	1066	1092	1161	1206	1281	1308	1335
NE	S	C	C	G	A	C	C	G	C	G	A	C	A	C	A	T
CE	R	Y	C	R	R	C	S	R	C	G	A	C	A	C	A	T
SW	G	C	Y	G	R	Y	S	G	Y	R	C	Y	G	G	R	C
	1344	1536	1548	1555	1563	1587	1590	1607	1626	1638	1671	1713	1834	1881	2085	2103
NE	C	A	R	C	G	G	C	C	A	G	C	C	C	R	C	K
CE	C	R	R	C	G	G	C	Y	A	G	Y	C	C	R	M	T
SW	G	R	G	T	R	R	S	C	G	R	C	Y	Y	R	C	T

Variations within group are listed as degenerate bases. Y: C/T, R: A/G, S: C/G, M: A/C, K: G/T. Variations that are identical between NE and CE groups, but different from SW group are indicated by gray shading.

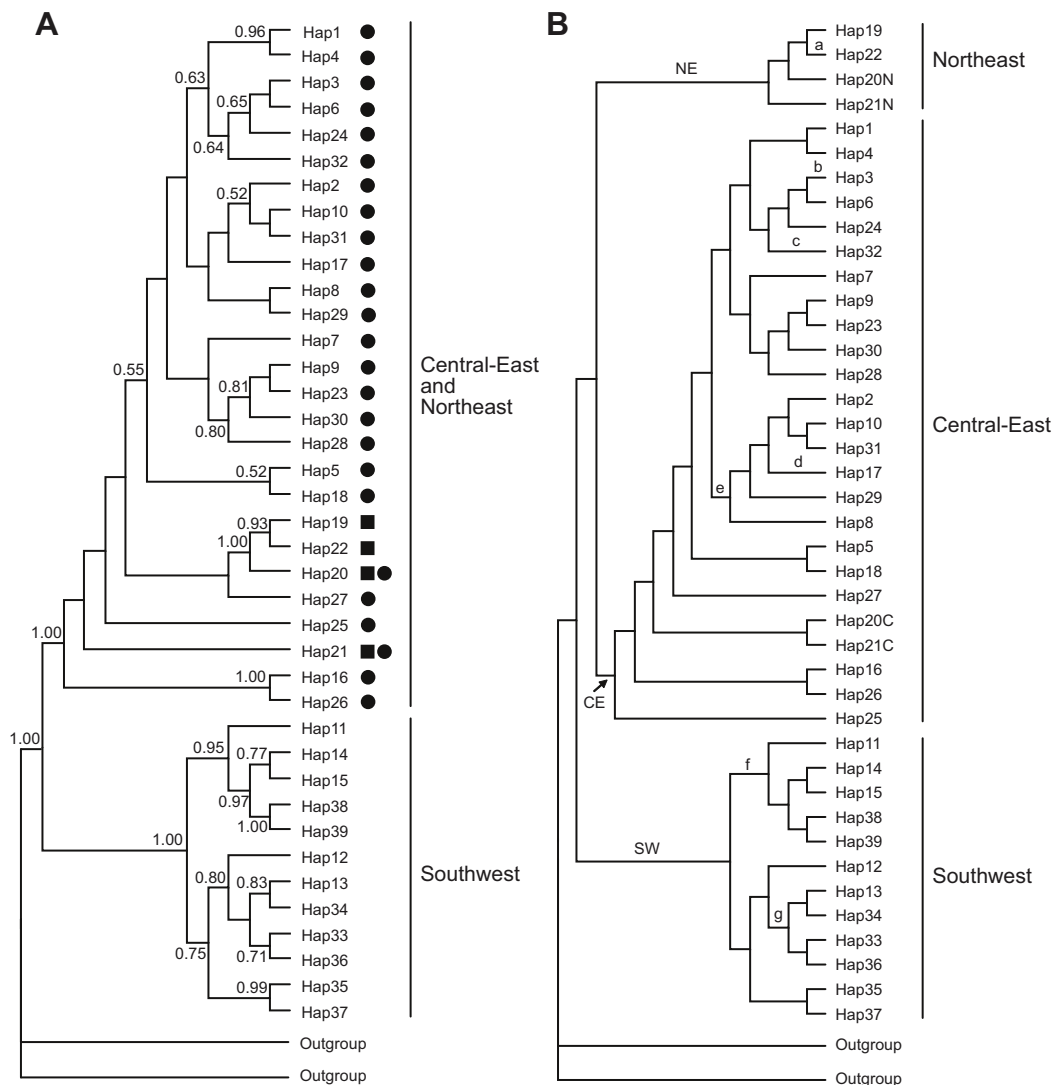


Fig. 4. *R. ferrumequinum* phylogenetic trees. (A) The Bayes phylogenetic tree of the *ZBED1* gene of *R. ferrumequinum*. The gene tree was based on complete *ZBED1* CDS. Posterior probabilities over 0.50 are shown on tree branches. Squares and circles indicate haplotypes that belong to the Northeast group and the Central-East group, respectively. The haplotypes shared between the Northeast and the Central-East groups are indicated by both squares and circles. (B) The phylogenetic tree of *R. ferrumequinum*. The topologic relationship among the Northeast group, the Central-East group and the Southwest group is based on previous mtDNA phylogenetic results (Sun et al., 2013). The inner relationship within each group was constructed by MrBayes 3.2.0 using *ZBED1* CDS in this study. Hap20 and Hap21, marked with 'N' and 'C', are haplotypes shared between the Northeast and the Central-East groups, respectively. Unlike haplotypes from the Northeast and the Central-East groups, which form one clade labeled with Central-East and Northeast in the gene tree (A), the haplotypes from the Northeast and the Central-East groups formed two separate clades in the species tree (B).

The discrete model (M3) with $K=3$ site classes suggested that 2.067% of sites were under positive selection with $\omega_2=1.00949$ and identified 10 amino acids under positive selection at 100% probability. The LRT statistic of M3($K=3$)-M0 comparison was significant ($2\Delta l=45.62$, d.f.=4, $P<0.001$).

We used clade models (branch-site model C) to test for potential divergent selection pressure among our three focal groups (Table 6). We first applied a multi-clade model C assuming three partitions: Northeast group, Central-East group and Southwest group. Under this model, which we call 'model $C_{CE\&NE}$ ', a small proportion of the dataset (only 1.819%) evolved under divergent selective constraint across the three partitions, with a ω ratio less than 1 along the SW branches [$\omega_{2(SW)}=0.00000$], above 1 along the Northeast group [$\omega_{2(NE)}=2.07667$] and slightly higher than 1 along the Central-East group [$\omega_{2(CE)}=1.07229$]. Then we used model C with either the

Northeast group ('model C_{NE} ') or the Central-East group ('model C_{CE} ') as the foreground partition and all others comprised the background partition. Using model C_{NE} , the ω ratio of the Northeast group was estimated to be 2.83291, whereas under model C_{CE} , the ω ratio of the Central-East group was less than 1 [$\omega_{2(CE)}=0.59606$]. LRT statistics suggested model $C_{CE\&NE}$ fits the data better compared with model C_{NE} and model C_{CE} . The comparison between model $C_{CE\&NE}$ and M1a was not statistically significant, but the comparison between model $C_{CE\&NE}$ and M2a_rel was statistically significant. We also compared model C_{CE} and model C_{NE} versus M1a and M2a_rel, respectively; neither of these comparisons were statistically significant, suggesting neither model C_{CE} nor model C_{NE} fit the data better than the null models. These results suggested that model $C_{CE\&NE}$ was more suitable for the data, and the Northeast and Central-East groups were under positive selection.

Table 3. Positive selection analyses of the *ZBED1* gene based on branch models

Branch model	Estimates of parameters	<i>l</i>	Likelihood ratio test (LRT)		
			2Δ <i>l</i>	d.f.	<i>P</i> -value
M0: one ratio	$\omega=0.01926$	−3430.70	–	–	–
Free ratio	–	−3400.25	–	–	–
Branch model (two ratio)					
Branch a	$\omega_0=0.01813, \omega_1=999.00000$	−3428.73	–	–	–
Branch b	$\omega_0=0.01812, \omega_1=999.00000$	−3428.74	–	–	–
Branch c	$\omega_0=0.01812, \omega_1=999.00000$	−3428.77	–	–	–
Branch d	$\omega_0=0.01587, \omega_1=999.00000$	−3425.16	–	–	–
Branch e	$\omega_0=0.01812, \omega_1=999.00000$	−3428.76	–	–	–
Branch f	$\omega_0=0.01814, \omega_1=999.00000$	−3429.01	–	–	–
Branch g	$\omega_0=0.01821, \omega_1=999.00000$	−3429.18	–	–	–
Branch NE	$\omega_0=0.01885, \omega_1=2.01765$	−3431.55	–	–	–
Branch CE	$\omega_0=0.01928, \omega_1=1.48366$	−3431.10	–	–	–
Branch model (two ratio, $\omega_1=1$)					
Branch a	$\omega_0=0.01811, \omega_1=1.00000$	−3428.84	–	–	–
Branch b	$\omega_0=0.01812, \omega_1=1.00000$	−3428.85	–	–	–
Branch c	$\omega_0=0.01812, \omega_1=1.00000$	−3428.87	–	–	–
Branch d	$\omega_0=0.01585, \omega_1=1.00000$	−3425.07	–	–	–
Branch e	$\omega_0=0.01812, \omega_1=1.00000$	−3428.87	–	–	–
Branch f	$\omega_0=0.01815, \omega_1=1.00000$	−3429.08	–	–	–
Branch g	$\omega_0=0.01821, \omega_1=1.00000$	−3429.26	–	–	–
Branch NE	$\omega_0=0.01885, \omega_1=1.00000$	−3431.55	–	–	–
Branch CE	$\omega_0=0.01926, \omega_1=1.00000$	−3430.70	–	–	–
LRT of variable ω values among branches					
Free ratio versus M0			60.90	78	0.924
LRT of ω at specific lineages (two ratio versus one ratio)					
Branch a			3.94	1	0.047
Branch b			3.92	1	0.048
Branch c			3.86	1	0.049
Branch d			11.08	1	0.001
Branch e			3.88	1	0.049
Branch f			3.38	1	0.066
Branch g			3.04	1	0.081
Branch NE			1.70	1	0.192
Branch CE			0.80	1	0.371
LRT of ω at specific lineages (two ratio versus two ratio, $\omega_1=1$)					
Branch a			0.22	1	0.639
Branch b			0.22	1	0.639
Branch c			0.20	1	0.655
Branch d			0.18	1	0.671
Branch e			0.22	1	0.639
Branch f			0.14	1	0.708
Branch g			0.16	1	0.689
Branch NE			0.00	1	1.000
Branch CE			0.80	1	0.371

The branches that were defined as the foreground branches in the two-ratio model are shown in Fig. 4B.

DISCUSSION

Mammalian hibernators experience physiological extremes, e.g. ischemia, muscle disuse and hypothermia, that are lethal to non-hibernators but have no deleterious effects on hibernators. This could suggest the existence of underlying mechanisms that allow hibernators to withstand these physiological extremes. To date, several possible protective mechanisms have been proposed (Carey et al., 2000; Cerri et al., 2009; Lei et al., 2014) and among them, increased cell proliferation appears to represent a major protective mechanism to compensate for increased apoptotic cells during hibernation (Cerri et al., 2009).

In this study, using *R. ferrumequinum* as a model system, we evaluated the expression and adaptive evolution of an important transcription factor (*ZBED1*) that plays a key role in the control of cell proliferation (Matsukage et al., 2008). Gene expression analyses showed that out of the five tissues analyzed, the *ZBED1* gene is overexpressed only in the brain and skeletal muscle tissue

during deep hibernation when compared with pre-hibernation and post-hibernation. This tissue-specific overexpression may suggest that these tissues have a high level of cell proliferation. The increased expression of *ZBED1* in the brain observed in this study is consistent with the study of Cerri et al. (2009), in which increased cell proliferation in the brain of a species of hibernating frog (*Rana esculenta*) is demonstrated. In addition, an increased cellular proliferation in tests in some hibernators, e.g. ground squirrels and woodchucks, is suggested to account for their full sexual activity during hibernation (Wimsatt, 1969). Increased cell proliferation in certain tissues found in these studies and our own study might suggest tissue heterogeneity, because many other specific tissues (e.g. lymphocytes, liver and hippocampus) are suggested to undergo a reduced cellular proliferation during hibernation (Shivatcheva and Hadjioloff, 1987; Kruman, 1992; Kiss et al., 2011; Popov et al., 2011). Different tissues might suffer different pressures during hibernation and hence might need variable protective mechanisms.

Table 4. Positive selection analyses of the *ZBED1* gene based on branch-site models

Branch-site model	Estimates of parameters	<i>l</i>	Test	Likelihood ratio test (LRT)		
				$2\Delta l$	d.f.	<i>P</i> -value
M1a: nearly neutral	$p_0=0.97925, p_1=0.02075$ $\omega_0=0.00000, \omega_1=1.00000$	–3407.48	–	–	–	–
Model A (alternative hypothesis) for branch NE	$p_0=0.97924, p_1=0.02075, p_{2a}=0.00000, p_{2b}=0.00000$ Background: $\omega_0=0.00000, \omega_1=1.00000, \omega_{2a}=0.00000, \omega_{2b}=0.00000$ Foreground: $\omega_0=0.00000, \omega_1=1.00000, \omega_{2a}=1.00000, \omega_{2b}=1.00000$	–3407.89	1	0.82	2	>0.05
Model A (null hypothesis) for branch NE	$p_0=0.97925, p_1=0.02075, p_{2a}=0.00000, p_{2b}=0.00000$ Background: $\omega_0=0.00000, \omega_1=1.00000, \omega_{2a}=0.00000, \omega_{2b}=0.00000$ Foreground: $\omega_0=0.00000, \omega_1=1.00000, \omega_{2a}=1.00000, \omega_{2b}=1.00000$	–3407.89	2	0.00	1	>0.05
Model A (alternative hypothesis) for branch CE	$p_0=0.91841, p_1=0.01947, p_{2a}=0.06083, p_{2b}=0.00129$ Background: $\omega_0=0.00000, \omega_1=1.00000, \omega_{2a}=0.00000, \omega_{2b}=1.00000$ Foreground: $\omega_0=0.00000, \omega_1=1.00000, \omega_{2a}=3.16380, \omega_{2b}=3.16380$	–3407.89	1	0.82	2	>0.05
Model A (null hypothesis) for branch CE	$p_0=0.91672, p_1=0.01943, p_{2a}=0.06252, p_{2b}=0.00133$ Background: $\omega_0=0.00000, \omega_1=1.00000, \omega_{2a}=0.00000, \omega_{2b}=1.00000$ Foreground: $\omega_0=0.00000, \omega_1=1.00000, \omega_{2a}=1.00000, \omega_{2b}=1.00000$	–3407.89	2	0.00	1	>0.05

The branches that were defined as the foreground branches are shown in Fig. 4B.

Given the stress that the brain suffers during hibernation, such as ischemia-induced oxidative stress and thermal stress (Carey et al., 2003; Dave et al., 2012), the increased *ZBED1* expression in the brain during deep hibernation observed in this study could be associated with cell proliferation and hence may be helpful to compensate for cell death and the onset of neurological damages. Further analyses showed that the expression of the gene in the skeletal muscle is consistently higher than that of the other four tissues used in this study. The overexpression of the *ZBED1* gene in skeletal muscle tissue might imply a high level of cell proliferation. The possible cell proliferation might partly account for the lack of muscle atrophy in hibernators after extended periods of disuse during hibernation. Inactivity in humans, such as confined bed rest, weightlessness or limb immobilization, can lead to atrophy of skeletal muscle, loss of muscle tone and impaired strength (Harlow

et al., 2001). However, in hibernating animals, such as ground squirrels and bats, although their skeletal muscle mass is reduced by 14–65% depending on muscle type and species, neither atrophy nor dysfunction is found in their skeletal muscle (Steffen et al., 1991; Wickler et al., 1991). The possible increase of cell proliferation in skeletal muscle could therefore help to maintain the function of skeletal muscle during hibernation.

Phylogenetic analyses of the *ZBED1* gene showed a strong genetic divergence between the Northeast group and the Southwest group of *R. ferrumequinum*, which represent hibernating and non-hibernating groups, respectively. This would imply a functional divergence between them. Positive selection analyses further showed some evidence of the adaptive evolution of the *ZBED1* gene. The branch model detected five positive selected branches, which were found to be restricted to the Northeast and the

Table 5. Positive selection analyses of the *ZBED1* gene based on site models

Model	Estimates of parameters	<i>l</i>	Likelihood ratio test (LRT)			Positively selected sites
			$2\Delta l$	d.f.	<i>P</i> -value	
M0: one ratio	$\omega=0.01926$	–3430.70	–	–	–	None
M1a: nearly neutral (K=2)	$p_0=0.97925 (p_1=0.02075)$ $\omega_0=0.00000, \omega_1=1.00000$	–3407.48	–	–	–	Not allowed
M2a: Positive selection (K=3)	$p_0=0.97930, p_1=0.01783$ ($p_2=0.00287$) $\omega_0=0.00000,$ $\omega_1=1.00000, \omega_2=1.04714$	–3407.89	–	–	–	324A (0.724)
M2a_rel	$p_0=0.75622, p_1=0.02075$ ($p_2=0.22303$) $\omega_0=0.00000,$ $\omega_1=1.00000, \omega_2=0.00000$	–3407.48	–	–	–	None
M3: discrete (K=3)	$p_0=0.15772, p_1=0.82161$ ($p_2=0.02067$) $\omega_0=0.00000,$ $\omega_1=0.00000, \omega_2=1.00949$	–3407.89	–	–	–	120A (1.000), 197A (1.000), 228A (1.000), 243T (1.000), 312G (1.000), 324A (1.000), 327A (1.000), 356G (1.000), 536A (1.000), 701F (1.000)
M7: beta	$p=0.00945, q=0.22253$	–3414.74	–	–	–	None
M8: beta & $\omega > 1$	$p_0=0.97934, p=0.00500,$ $q=2.75586, (p_1=0.02066),$ $\omega=1.00952$	–3407.89	–	–	–	197A (0.535), 243T (0.528), 324A (0.932), 356G (0.525), 536A (0.534)
LRT of variable ω values among sites						
M0 versus M3(K=3)		–	45.62	4	<0.001	–
M1a versus M2a		–	0.82	2	0.664	–
M7 versus M8		–	13.70	2	0.001	–

Note: numbers in the brackets following amino acid sites are posterior probability of positively selected sites. The reference sequence is Hap39.

Table 6. Positive selection analyses of the *ZBED1* gene based on clade models

Clade model	Estimates of parameters	<i>I</i>	Likelihood ratio test (LRT)		
			$2\Delta l$	d.f.	<i>P</i> -value
Model $C_{CE\&NE}$	$p_0=0.97517, p_1=0.00664$ ($p_2=0.01819$) $\omega_0=0.00000, \omega_1=1.00000, \omega_{2(SW)}=0.00000, \omega_{2(NE)}=2.07667,$ $\omega_{2(CE)}=1.07229$	–3403.76	–	–	–
Model C_{CE}	$p_0=0.97003, p_1=0.01458$ ($p_2=0.01540$) $\omega_0=0.00000, \omega_1=1.00000, \omega_{2(SW-NE)}=0.00000, \omega_{2(CE)}=0.59606$	–3406.50	–	–	–
Model C_{NE}	$p_0=0.97881, p_1=0.01060$ ($p_2=0.01059$) $\omega_0=0.00000, \omega_1=1.00000, \omega_{2(SW-CE)}=0.72245, \omega_{2(NE)}=2.83291$	–3407.00	–	–	–
LRT of variable ω values among sites and branches					
Model $C_{CE\&NE}$ versus M1a		–	7.44	4	0.114
Model $C_{CE\&NE}$ versus M2a_rel		–	7.44	2	0.024
Model $C_{CE\&NE}$ versus model C_{CE}		–	5.48	1	0.019
Model $C_{CE\&NE}$ versus model C_{NE}		–	6.48	1	0.011
Model C_{CE} versus M1a		–	1.96	3	0.581
Model C_{CE} versus M2a_rel		–	1.96	1	0.162
Model C_{NE} versus M1a		–	0.96	3	0.811
Model C_{NE} versus M2a_rel		–	0.96	1	0.327

The three clades (Northeast, Central-East and Southwest) are shown in Fig. 4B.

Central-East groups that are dominated by hibernating individuals. Under the site model, several positively selected sites were detected, of which, one site, 324A, was found to be with a high probability under positive selection. The amino acid 324A is putatively located in the ribonuclease H-like catalytic domain in the protein structure of *ZBED1* (Mitchell et al., 2015). Our clade model supports the existence of divergent selection pressures of the *ZBED1* gene among the three mtDNA groups. Estimates of ω were >1 for $\sim 2\%$ of sites when the Northeast and Central-East groups ($\omega_{NE}=2.07667$, $\omega_{CE}=1.07229$) were defined as the foreground clades. This may indicate a strong positive selective pressure on the Northeast group and a slight positive selective pressure on the Central-East group. Nevertheless, in the Southwest group, we detected no evidence for positive selection. These findings remained unchanged when the *ZBED1* phylogenetic tree (Fig. 4A) was used for our positive selection analyses (data not shown). Identification of the positively selected branches and positive selective pressure on the Northeast and Central-East groups support our prediction that adaptive evolution of *ZBED1* might occur in the hibernating groups of *R. ferrumequinum*.

In this study, using *R. ferrumequinum* as a model system, we investigated the expression and adaptive evolution of the *ZBED1* gene, an important cell proliferation-related transcription factor, and found a potential role of the *ZBED1* gene in hibernation. We found an overexpression of the *ZBED1* gene only in the brain and skeletal muscle, and detected some evidence of adaptive evolution of this gene in hibernating groups of *R. ferrumequinum*. Our results suggest that *ZBED1* may be a potential candidate gene that regulates cell proliferation for hibernators to face the physiological extremes of hibernation.

Acknowledgements

We are thankful to Hongjun Lin and Bo Luo for their great contributions to samples collection and Yuyang Hao for her help in the experiments. We are grateful to Katie Andrea Solari for her help in language revision.

Competing interests

The authors declare no competing or financial interests.

Author contributions

J.F., Y.W. and K.S. conceived and designed the experiments. Y.X., Y.W., H.W., T.J., A.L., X.H., X.Y. and L.S. collected the samples and performed the experiments. J.F. contributed reagents, materials and analysis tools. Y.X. wrote the paper. All authors read and approved the final manuscript.

Funding

This study was supported by the National Natural Science Foundation of China [grant numbers 91131003, 31270414, 31370399].

Supplementary information

Supplementary information available online at <http://jeb.biologists.org/lookup/suppl/doi:10.1242/jeb.133272/-DC1>

References

- Aulagnier, S., Hutson, A. M., Spitzenberger, F., Juste, J., Karataş, A., Palmeirim, J. and Paunovic, M. (2008). *Rhinolophus ferrumequinum*. The IUCN Red List of Threatened Species 2008: e.T19517A8947355.
- Bielawski, J. P. and Yang, Z. (2004). A maximum likelihood method for detecting functional divergence at individual codon sites, with application to gene family evolution. *J. Mol. Evol.* **59**, 121–132.
- Carey, H. V., Sills, N. S. and Gorham, D. A. (1999). Stress proteins in mammalian hibernation. *Am. Zool.* **39**, 825–835.
- Carey, H. V., Frank, C. L. and Seifert, J. P. (2000). Hibernation induces oxidative stress and activation of NK-kappaB in ground squirrel intestine. *J. Comp. Physiol. B Biochem. Syst. Environ. Physiol.* **170**, 551–559.
- Carey, H. V., Andrews, M. T. and Martin, S. L. (2003). Mammalian hibernation: cellular and molecular responses to depressed metabolism and low temperature. *Physiol. Rev.* **83**, 1153–1181.
- Cerri, S., Bottiroli, G., Bottone, M. G., Barni, S. and Bernocchi, G. (2009). Cell proliferation and death in the brain of active and hibernating frogs. *J. Anat.* **215**, 124–131.
- Dave, K. R., Christian, S. L., Perez-Pinzon, M. A. and Drew, K. L. (2012). Neuroprotection: lessons from hibernators. *Comp. Biochem. Phys. B Biochem. Mol. Biol.* **162**, 1–9.
- Harlow, H. J., Lohuis, T., Beck, T. D. I. and Iuzzo, P. A. (2001). Muscle strength in overwintering bears. *Nature* **409**, 997.
- Hirose, F., Yamaguchi, M., Nishida, Y., Masutani, M., Miyazawa, H., Hanaoka, F. and Matsukage, A. (1991). Structure and expression during development of *Drosophila melanogaster* gene for DNA polymerase alpha. *Nucleic Acids. Res.* **19**, 4991–4998.
- Hirose, F., Yamaguchi, M., Handa, H., Inomata, Y. and Matsukage, A. (1993). Novel 8-base pair sequence (*Drosophila* DNA replication-related element) and specific binding factor involved in the expression of *Drosophila* genes for DNA polymerase alpha and proliferating cell nuclear antigen. *J. Biol. Chem.* **268**, 2092–2099.
- Kandror, O. and Goldberg, A. L. (1997). Trigger factor is induced upon cold shock and enhances viability of *Escherichia coli* at low temperatures. *Proc. Natl. Acad. Sci. USA* **94**, 4978–4981.
- Kiss, A. J., Muir, T. J., Lee, R. E. Jr. and Costanzo, J. P. (2011). Seasonal variation in the hepatoproteome of the dehydration- and freeze-tolerant wood frog, *Rana sylvatica*. *Int. J. Mol. Sci.* **12**, 8406–8414.
- Kruman, I. I. (1992). Comparative analysis of cell replacement in hibernators. *Comp. Biochem. Physiol. A Physiol.* **101**, 11–18.
- Lei, M., Dong, D., Mu, S., Pan, Y.-H. and Zhang, S. (2014). Comparison of brain transcriptome of the greater horseshoe bats (*Rhinolophus ferrumequinum*) in active and torpid episodes. *PLoS ONE* **9**, e107746.
- Librado, P. and Rozas, J. (2009). DnaSP v5: a software for comprehensive analysis of DNA polymorphism data. *Bioinformatics* **25**, 1451–1452.

- Livak, K. J. and Schmittgen, T. D. (2001). Analysis of relative gene expression data using real-time quantitative PCR and the 2(-Delta Delta C(T)) method. *Methods* **25**, 402–408.
- Martin, D. P., Lemey, P., Lott, M., Moulton, V., Posada, D. and Lefevre, P. (2010). RDP3: a flexible and fast computer program for analyzing recombination. *Bioinformatics* **26**, 2462–2463.
- Matsukage, A., Hirose, F., Yoo, M. and Yamaguchi, M. (2008). The DRE/DREF transcriptional regulatory system: a master key for cell proliferation. *Biochim. Biophys. Acta* **1779**, 81–89.
- Mitchell, A., Chang, H.-Y., Daugherty, L., Fraser, M., Hunter, S., Lopez, R., McAnulla, C., McMenamin, C., Nuka, G., Pesseat, S. et al. (2015). The InterPro protein families database: the classification resource after 15 years. *Nucleic Acids Res.* **43**, D213–D221.
- Murrell, B., Wertheim, J. O., Moola, S., Weighill, T., Scheffler, K. and Pond, S. L. K. (2012). Detecting individual sites subject to episodic diversifying selection. *PLoS Genet.* **8**, e1002764.
- Ohno, K., Hirose, F., Sakaguchi, K., Nishida, Y. and Matsukage, A. (1996). Transcriptional regulation of the *Drosophila* CycA gene by the DNA replication-related element (DRE) and DRE binding factor (DREF). *Nucleic Acids Res.* **24**, 3942–3946.
- Phuong Thao, D. T., Ida, H., Yoshida, H. and Yamaguchi, M. (2006). Identification of the *Drosophila* skpA gene as a novel target of the transcription factor DREF. *Exp. Cell Res.* **312**, 3641–3650.
- Pond, S. L. K. and Frost, S. D. (2005a). Not so different after all: a comparison of methods for detecting amino acid sites under selection. *Mol. Biol. Evol.* **22**, 1208–1222.
- Pond, S. L. K. and Frost, S. D. W. (2005b). Datamonkey: rapid detection of selective pressure on individual sites of codon alignments. *Bioinformatics* **21**, 2531–2533.
- Pond, S. L. K. and Muse, S. V. (2005). HyPhy: hypothesis testing using phylogenies. In *Statistical Methods in Molecular Evolution* (ed. R. Nielsen), pp. 125–181. New York: Springer.
- Popov, V. I., Kraev, I. V., Ignat'ev, D. A. and Stewart, M. G. (2011). Suspension of mitotic activity in dentate gyrus of the hibernating ground squirrel. *Neural Plast.* **2011**, 867525.
- Posada, D. and Crandall, K. (2005). *Modeltest 3.7. Program Distributed by the Author*. Spain: Universidad de Vigo.
- Ronquist, F. and Huelsenbeck, J. P. (2003). MrBayes 3: bayesian phylogenetic inference under mixed models. *Bioinformatics* **19**, 1572–1574.
- Ryu, J.-R., Choi, T.-Y., Kwon, E.-J., Lee, W.-H., Nishida, Y., Hayashi, Y., Matsukage, A., Yamaguchi, M. and Yoo, M.-A. (1997). Transcriptional regulation of the *Drosophila*-raf proto-oncogene by the DNA replication-related element (DRE)/DRE-binding factor (DREF) system. *Nucleic Acids Res.* **25**, 794–799.
- Sawado, T., Hirose, F., Takahashi, Y., Sasaki, T., Shinomiya, T., Sakaguchi, K., Matsukage, A. and Yamaguchi, M. (1998). The DNA replication-related element (DRE)/DRE-binding factor system is a transcriptional regulator of the *Drosophila* E2Fgene. *J. Biol. Chem.* **273**, 26042–26051.
- Shivatcheva, T. M. and Hadjioloff, A. I. (1987). Seasonal involution of gut-associated lymphoid tissue of the European ground squirrel. *Dev. Comp. Immunol.* **11**, 791–799.
- Sonna, L. A., Fujita, J., Gaffin, S. L. and Lilly, C. M. (2002). Invited review: effects of heat and cold stress on mammalian gene expression. *J. Appl. Physiol.* **92**, 1725–1742.
- Steffen, J. M., Koebel, D. A., Musacchia, X. J. and Milsom, W. K. (1991). Morphometric and metabolic indices of disuse in muscles of hibernating ground squirrels. *Comp. Biochem. Phys. B Comp. Biochem.* **99**, 815–819.
- Sun, K., Luo, L., Kimball, R. T., Wei, X., Jin, L., Jiang, T., Li, G. and Feng, J. (2013). Geographic variation in the acoustic traits of greater horseshoe bats: testing the importance of drift and ecological selection in evolutionary processes. *PLoS ONE* **8**, e70368.
- Takahashi, Y., Yamaguchi, M., Hirose, F., Cotterill, S., Kobayashi, J., Miyajima, S. and Matsukage, A. (1996). DNA replication-related elements cooperate to enhance promoter activity of the *Drosophila* DNA polymerase alpha 73-kDa subunit gene. *J. Biol. Chem.* **271**, 14541–14547.
- Tamura, K., Stecher, G., Peterson, D., Filipksi, A. and Kumar, S. (2013). MEGA6: molecular evolutionary genetics analysis version 6.0. *Mol. Biol. Evol.* **30**, 2725–2729.
- Tsuchiya, A., Inoue, Y. H., Ida, H., Kawase, Y., Okudaira, K., Ohno, K., Yoshida, H. and Yamaguchi, M. (2007). Transcriptional regulation of the *Drosophila* rfc1 gene by the DRE-DREF pathway. *FEBS J.* **274**, 1818–1832.
- Wang, L. C., Lee, T., Fregley, M. and Blatteis, C. (1996). Torpor and hibernation in mammals: metabolic, physiological, and biochemical adaptations. In *Handbook of Physiology: Environmental Physiology* (ed. J. R. Pappenheimer, M. J. Fregly and C. M. Blatties), pp. 507–532. New York: Oxford University Press.
- Weadick, C. J. and Chang, B. S. W. (2012a). Complex patterns of divergence among green-sensitive (RH2a) African cichlid opsins revealed by Clade model analyses. *BMC Evol. Biol.* **12**, 206.
- Weadick, C. J. and Chang, B. S. W. (2012b). An improved likelihood ratio test for detecting site-specific functional divergence among clades of protein-coding genes. *Mol. Biol. Evol.* **29**, 1297–1300.
- Wickler, S. J., Hoyt, D. F. and Van Breukelen, F. (1991). Disuse atrophy in the hibernating golden-mantled ground squirrel, *Spermophilus lateralis*. *Am. J. Physiol.* **261**, R1214–R1217.
- Wimsatt, W. A. (1969). Some interrelations of reproduction and hibernation in mammals. In *Dormancy and Survival* (ed. A. H. W. Woolhouse), pp. 511–549. London: Cambridge University Press.
- Worthington Wilmer, J. and Barratt, E. (1996). A non-lethal method of tissue sampling for genetic studies of chiropterans. *BAT Res. News* **37**, 1–3.
- Yang, Z. (2007). PAML 4: phylogenetic analysis by maximum likelihood. *Mol. Biol. Evol.* **24**, 1586–1591.

Supplementary information

Table S1. Primers of *ZBED1* and *β-actin* used for real time PCR.

Gene	Primer	Base sequence (5'- 3')	Tm (°C)	Products (bp)
<i>ZBED1</i>	Sense	TGACGTAGGTCCTGTTCTGGTT	60.0	238
	Anti-sense	CTCATCTGCGATGGGCTGT		
<i>β-actin</i> *	Sense	GACCTCTATGCCAACACAG	60.0	190
	Anti-sense	CATCTGCTGGAAGGTGGAC		

*Primer pair of *β-actin* was obtained in Chen et al. 2008.

Table S2. Sample information used for phylogenetic and positive selection analyses. The sampling sites and their corresponding mtDNA clades are shown. NE, Northeast group; CE, Central-East group; SW, Southwest group.

Sites No.	Sites	Evolutionary Group	Location		Samples No.
			Latitude	Longitude	
1	Ji'an, Jilin	NE	41°03'	125°50'	JL07, JL09, JL10, JL11, JL12, JL13
2	Shenyang, Liaoning	NE	41°48'	123°23'	LN1307, LN1308, LN1309, LN1310, LN1344
3	Fangshan, Beijing	CE	39°43'	115°59'	BJ1311, BJ1312, BJ1315, BJ1316, BJ1317
4	Jinan, Shandong	CE	36°43'	117°07'	SD19, SD20
5	Feixian, Shandong	CE	35°08'	117°44'	SD1185, SD1188, SD1189
6	Datong, Shanxi	CE	40°03'	113°19'	SX0827, SX0830, SX0831
7	Lantian, Shaanxi	CE	34°04'	109°24'	SXi1216, SXi1217, SXi1218, SXi1220, SXi1221
8	Anyang, Henan	CE	35°47'	113°56'	HeN1201, HeN1202, HeN1204, HeN1208, HeN1211
9	Chaohu, Anhui	CE	31°57'	117°52'	AH0801
10	Lu'an, Anhui	CE	31°22'	116°12'	AH1002, AH1004
11	Tianshui, Gansu	SW	34°20'	106°06'	GS1005, GS1008, GS1009, GS1011
12	Kunming, Yunnan	SW	24°30'	102°20'	YN21, YN07205
13	Dali, Yunnan	SW	25°20'	100°07'	YN22, YN23, YN24

Table S3. 39 *ZBED1* haplotypes and their corresponding individuals (alleles). Different alleles from each individual are distinguished by adding ‘A’ or ‘B’ tags to their individual identifiers.

Haplotype	Allele	Haplotype	Allele	Haplotype	Allele
Hap 1	AH0801A, SX0827A	Hap 14	GS1011A	Hap 27	SD1189B
Hap 2	AH0801B, AH1002B, BJ1317A, HeN1208A, SD1185A, SD1188A, Sxi1218	Hap 15	GS1011B	Hap 28	SX0830A
Hap 3	AH1002A	Hap 16	HeN1202A	Hap 29	SX0831A
Hap 4	AH1004A	Hap 17	HeN1204A	Hap 30	SX0831B
Hap 5	AH1004B	Hap 18	HeN1204B	Hap 31	Sxi1216
Hap 6	BJ1311A, BJ1312A, BJ1315B, HeN1201B, Sxi1220B	Hap 19	JL07, JL09, JL11B, JL12, JL13B, LN1307, LN1308, LN1309, LN1310, LN1344	Hap 32	Sxi1220A
Hap 7	BJ1311B, BJ1317B, HeN1201A, HeN1208B, HeN1211	Hap 20	JL10, SD1189A	Hap 33	YN21A
Hap 8	BJ1312B	Hap 21	JL11A, SD19, Sxi1217	Hap 34	YN21B
Hap 9	BJ1315A, HeN1202B, Sxi1221	Hap 22	JL13A	Hap 35	YN22A
Hap 10	BJ1316	Hap 23	SD20A	Hap 36	YN22B
Hap 11	GS1005A, GS1009	Hap 24	SD20B	Hap 37	YN23, YN24
Hap 12	GS1005B	Hap 25	SD1185B	Hap 38	YN07205A
Hap 13	GS1008	Hap 26	SD1188B, SX0827B, SX0830B	Hap 39	YN07205B

Table S4. The positive selection analyses of the *ZBED1* gene based on SLAC, FEL, REL, MEME and FUBAR methods.

Codon	SLAC		FEL		REL		MEME		FUBAR	
	dN-dS	p-value	dN-dS	p-value	dN-dS	Bayes factor	ω^+	p-value	dN-dS	Post. Pr.
120	10.974	0.667	33.867	0.491	-	-	1.759	0.487	-	-
197	10.974	0.667	34.305	0.483	-	-	1.331	0.485	-	-
228	-	-	-	-	-	-	102.699	0.437	-	-
243	10.941	0.669	30.806	0.511	-	-	1.402	0.507	-	-
312	10.962	0.668	31.473	0.505	-	-	1.710	0.490	-	-
324	54.870	0.132	166.558	0.125	5.583	4.726E+06*	7.018	0.218	3.233	0.971*
327	10.974	0.667	34.068	0.292	-	-	1.825	0.280	-	-
356	10.717	0.683	29.944	0.531	-	-	1.623	0.500	-	-
536	10.974	0.667	34.292	0.483	-	-	1.794	0.484	-	-
701	10.228	0.715	37.965	0.276	-	-	1.545	0.320	-	-

*Statistically significant value.